PEG hydration and conformation in aqueous solution: Hints to macromolecular crowding

S. Di Fonzo[a], B. Bellich[b], A. Gamini[c], N. Quadri[c], A. Cesàro[a,c,*]

[a] Elettra Sincrotrone Trieste, Area Science Park, I-34149, Trieste, Italy
[b] Department of Life Sciences, University of Trieste, Via Giorgieri 1, 34127, Trieste, Italy
[c] Department of Chemical and Pharmaceutical Sciences, University of Trieste, Via Giorgieri 1, 34127, Trieste, Italy

HIGHLIGHTS

- Several anomalous features of PEG aqueous solutions depend on concentration.
- Water activity in PEG solutions measured by a dynamic approach diverges from equilibrium.
- Relaxation processes from Brillouin scattering data show discontinuity in semi-dilute solutions.
- Raman bands evidence changes in local and segmental conformations.
- Anomalous features are traced back to conformation and solvation changes upon PEG dilution.

ARTICLE INFO

Keywords:
PEG solution dehydration rate
PEG relaxation
PEG conformation markers

ABSTRACT

The molecular structural dynamics of PEG in aqueous solution has been addressed with a series of experimental data correlating macroscopic solution properties of PEG with structural and hydration properties at molecular level, by using thermodynamic, UV Brillouin and Raman spectroscopy data. Water activity measured in PEG 600 solutions by a novel dynamical calorimetry approach shows that data reveal some non-equilibrium process for dilute solutions. Brillouin scattering data on aqueous solutions in the UV range made possible the measurement of the viscoelastic relaxation of the system with a characteristic temperature, T_M, as precursor of the glass transition process at lower T, while at constant temperature, the addition of water to liquid PEG 600 first lead to a slight decrease and then to an increase in the solution viscoelastic relaxation consistent with the slowest polymer dynamics observed in the concentrated solution. Specific Raman bands corresponding to *trans* and *gauche* conformations of the C–C and C–O bonds and their sequences in the PEG chain have been identified and their relative intensities as a function of concentration evidence non-monotonous variations with a rather unusual concentration dependence for the frequency of C–O bonds in the range of physiological temperatures.

The heuristic result is that the extended time-space domains approach suggests an overall quasi-regular solution behavior of semidilute PEG, with opposite concentration dependence at low and at high water content, similar to discontinuities observed in excess thermodynamic properties and eutectic phase diagram. The crossover of these distinct behaviors occurs at the concentration close to that usually employed to mimic the cellular crowding in biomolecular systems, highlighting the interplay of water molecules in solute-solute interactions.

1. Introduction

Macromolecular crowding is a well-known phenomenon largely interpreted in terms of excluded volume effects, with poor evidence reported in favor of some “non-specific” interactions of the added co-solutes [1–4]. As a matter of fact, biopolymer environments in food and biology area are far from dilute systems and water molecules are mainly engaged in the surface hydration layers of biomolecules and biomacromolecules [5–10]. Many technological protocols require a drastic reduction of the water mobility, which is also believed to be at the basis of the most common action of biopreservants, like sugars, among which trehalose is by far the most effective [11–13]. Several reviews have been written on the comparison of protocols and results aiming at explaining the possible molecular mechanisms that give rise to the observed structure in crowding and dehydration. In particular, the question whether the crowding phenomenon is governed by an

* Corresponding author. Elettra Sincrotrone Trieste, Area Science Park, I-34149, Trieste, Italy.
E-mail address: attilio.cesaro@elettra.eu (A. Cesàro).

https://doi.org/10.1016/j.polymer.2019.05.004

enthalpy or an entropy contribution, continuously debated in the past literature, has been more recently investigated with an enthalpy stabilization effect observed on proteins in solution of glucose, dextran and poly (ethylene glycol) [14]. Still, the mere effect of the size difference between biomolecules and biomacromolecules is relevant for the thermodynamic (colligative) properties, inasmuch the basic Flory-Huggins model and excluded volume are concerned [15]. In addition, when high molecular mass components are involved, not only long-range interactions occur either intra-molecularly or inter-molecularly, but also the interplay of hydration water becomes a very complex phenomenon (for a review see Comez et al., [16]).

Among the compounds effective in crowding, the phenomenology of poly(ethylene glycol)-water system [17] seems particularly relevant in many technological areas (see for example refs. [18–20]). Aqueous PEG solution experiments suggested an extensive equilibrium hydration structure [21–24]), and, more or less explicitly, the hydration and conformational properties of PEGs until recently were reported in literature to be at the basis of its influence on collective hydration and macromolecular crowding [6,25,26]. These findings implement other macromolecular properties previously investigated by single-molecule force measurements [27] and surface-monolayer studies [28], as well as theoretical approaches [29,30].

A few molecular dynamics studies have been performed focusing on the features of the statistical conformation of PEG in aqueous solutions. Among the first investigations, Tasaki et al. performed MD simulation of a single PEG chain with low molecular weight (with degree of polymerization n = 16) focused on polymer conformation and water interaction, providing preliminary insights into the snapshots of single PEG molecules in solution [31]. Some years after, molecular dynamics simulations of aqueous solutions of PEG (n = 12) were carried out as a function of solution composition in order to investigate the dependence of polymer dynamics on the water content [32]. Hydrodynamic features of PEG (n = 9 to n = 158) and their dependence on the anisotropy of the chain globule at low molecular weight were studied by Pastor and coworkers [33,34], showing the substantial agreement with current polymer statistical theories.

While the solvent effect on polymer conformation is a known phenomenon studied also in our laboratory [35], less clear is the interplay between polymer conformation and solution composition and properties in the presence of H-bond asymmetry in solute-solvent interactions. More recent simulations on polymer configurations of high molecular weight PEG at 25% w/w [36] show that polymer configurations seem mainly determined by short-range interactions and water first solvation shell, allowing a quite large distribution of chain dimensions of the PEG coils. Indeed, the unusual hydrogen bonding features of PEG-water system was also taken as the rule for explaining the presence of the Flory-Huggins “lower critical solution temperature” [23,37], PEG molecules exhibiting a curious interplay between intra- and inter-molecular interactions [38,39]. Thus, the extraordinary solution properties of PEG have been ascribed to the fact that *gauche* conformers are more polar and offer two hydrogen bond acceptor sites with an oxygen-oxygen distance very close to that of bulk water [40].

However, a clear correlation between local and long-range collective properties seems to be still elusive [41], in particular, for the changes occurring in the full range of concentration. In the present work, a series of experimental data is provided with the aim of correlating macroscopic solution properties of PEG with structural and hydration properties at molecular level. The correlation between solvation and conformation effects is presented in different time-space domains, since the exploration of a large time-domain has been shown very useful in the identification of signals that can be regarded as precursors of crowding and of a glass transition temperature [13].

Thus, the results of the investigation of PEG hydration/conformation characteristics concern solution dehydration studies by isothermal calorimetry, conformation Raman Spectroscopy supported by molecular simulation studies, with parallel investigation of the changes in the structural relaxation by inelastic UV Brillouin scattering. The full range of concentrations explored is intended to cover in particular the pure liquid PEG and the semi-dilute solutions resembling those used for the crowded systems.

2. Materials and methods

2.1. Materials

Polyethylene glycol (PEG 600 - BioUltra 87333, PEG 1000 - BioUltra 81188, PEG 6000 – BioUltra 81255) were purchased from Sigma-Aldrich Co. (St. Louis, Missouri, USA) and used without further purification; all the solutes were classified with purity ≥99%. Melting temperature of PEG samples were T_m = 21, 42 and 63 °C (peak temperatures) for PEG 600, PEG 1000 and PEG 6000, respectively, and were determined by DSC measurement at 20 °C/min scanning rate (see Supplementary data Fig. S1).

The PEG solutions were prepared by using MilliQ water (Millipore Corporation, Bedford, Massachusetts). Filter paper (grade 93, particle retention 10 μm, Whatman International LTD, UK) was used as film support for calorimetric dehydration measurements. Solutions for IUVS and Raman experiments were prepared by weight, after PEG dehydration at 100 °C for 24 h, by directly dissolving the polymer in the UV-grade quartz cells (1 cm path length), in double distilled and deionized water.

In terms of monomer molar fraction x, the concentrations used in the spectroscopic experiments correspond to x = 0.1, 0.33 and 0.5, or to n_w = 9, 2 and 1 water molecules per number of oxyethylene units in the polymer. A table and a figure correlating the different concentration scales is reported in Supplementary data, Table S1 and Fig. S2.

2.2. Methods

2.2.1. Isothermal dehydration experiments by calorimetry

Samples of film solutions were all prepared following an internal standard technique [42]. Paper disks that fit the calorimetry pans (DSC) were obtained with a desktop hole puncher. The diameter and the thickness of a disk were respectively 5.9 mm (surface area of 27.3 mm^2) and 0.11 mm, according to the average size previously measured by more than 40 paper disks. Calorimetric measurements were carried out at constant temperature with a DSC 6 (PerkinElmer Instruments, Waltham, Massachusetts). The sample, consisting of a solution on a paper disk placed in an open aluminum pan, was weighed before the measurement and then rapidly introduced in the calorimetric chamber. A dry paper disk was placed in the reference pan, to compensate the heat capacity of the paper, although small. Experiments were carried out with three PEG samples (600, 1000 and 6000) and three amounts of loaded solutions (4, 8 and 12 mg, respectively). By comparing the accuracy of the experimental results, only the 12 mg samples have been reported. All the dehydration experiments were carried out in isothermal conditions at 20 °C for about 200 min under N_2 flux of 15 mL/min. Data were collected by the software Pyris 2000 (PerkinElmer Instruments LLC Version 3.8) and were processed using the software Origin®. All measurements were repeated in triplicates.

2.2.2. Inelastic ultraviolet scattering measurements (IUVS)

IUVS experiments were carried out at the BL10.2 beamline of the Elettra synchrotron radiation facility in Trieste [43]. Spectra were acquired at 220 nm. The radiation scattered by the sample in a nearly backscattering configuration (θ = 172°) was energy-analyzed by a normal incidence Czerny-Turner analyzer and detected by a Peltier-cooled CCD camera (13.5 × 13.5 μm^2 pixel size, 20% quantum efficiency). The overall relative energy resolution was set to $\Delta E/E \approx 3\ 10^{-6}$. The acquisition time for a single IUVS spectrum was of about 60 min.

The sample was placed in a UV-grade quartz cell, kept in thermal

contact with the cold finger of a cryostat and a resistive heater. For each sample, either polymer melts or water solutions, the temperature was varied in the range above the corresponding melting point up to 100 °C and monitored with a K-type thermocouple and electronically controlled with an accuracy of 0.5 °C. The entire system was placed in a moderate vacuum atmosphere in order to avoid spurious scattering from air and temperature gradients.

By limiting the spectral analysis to frequencies close to those corresponding to inelastic excitations, the spectrum was approximated by the convolution of the experimental resolution with the following function, which is the sum of a δ(ω)-function, accounting for spurious elastic scattering, and a Damped Harmonic Oscillator (DHO) function [44], accounting for the inelastic signal:

$$S(Q,\omega) = A\delta + B\frac{\omega_B^2(Q)\Gamma_B(Q)}{(\omega^2 - \omega_B^2(Q))^2 + \omega^2\Gamma_B(Q)} \quad (1)$$

where ω_B and Γ_B are the inelastic peak frequency and full width at half maximum (FWHM), respectively, while A and B are scaling factors. The data fitting procedure was based on a standard nonlinear least squares Levenberg-Marquardt algorithm [45].

2.2.3. Raman measurements

Measurements were performed with the Raman spectrometer placed at a branch-line of the beamline 10.2 of the Elettra synchrotron radiation laboratory in Trieste Italy. In the present case the source was a laser diode-pumped Nd:YAG laser delivering radiation at 266 nm. UV light was used in order to avoid sample auto-fluorescence, thus slightly improving the signal-to-noise ratio obtainable with visible light sources. Raman signal was detected by a spectrometer (TriVista 557, Princeton Instruments), equipped with a 1800 lines/mm flat holographic gratings optimized for UV radiation and collected by a nitrogen-cooled low-noise CCD detector (Spec-10, Princeton Instruments). Measurements were recorded with 1 min acquisition time in the 700-3500 cm^{-1} wavenumber range. The instrumental spectral resolution was set to 12 cm^{-1}. PEG pure liquid and solutions were measured in the liquid phase at T = 27, 57 and 87 °C. Sample temperature was controlled with 0.5 °C accuracy.

3. Results and discussion

3.1. Isothermal evaporation data

General shape of dehydration curves by calorimetry. The experimental dehydration curves of aqueous solutions from thin films measured by a novel isothermal calorimetric method follow a quite general trend. The theoretical model (scheme in Fig. S3) was developed to correctly evaluate the water activity measured by the calorimetric output (heat flow) which is function of the parameters affecting the process of dehydration, such as sample mass, temperature, nitrogen flux and other functional variables [42,46]. The validity of the model was verified by several experiments with water and aqueous solutions of glucose and trehalose [46] and corroborated by direct comparison with dehydration of $CaCl_2$ solutions [47]. Homogeneous solutions and gels have been shown to fall in this class provided that they satisfy the conditions of the theoretical model. In general, the rate of convective evaporation from a surface saturated with water can be considered constant if the surface dimension Σ remains constant and all the external conditions are constant, i.e., temperature (low is better), vapor phase relative humidity (very low is better), purge gas flow (medium-low is better).

The experimental results obtained for 12 mg loaded solutions of PEG 600 at six representative initial concentrations (2, 5, 10, 20, 30, 40% w/w) are reported in Fig. 1. Experiments with 4, 8 and 12 mg loaded water are also reported in Fig. 1 as a reference.

By following the theoretical basis and the experimental evidence

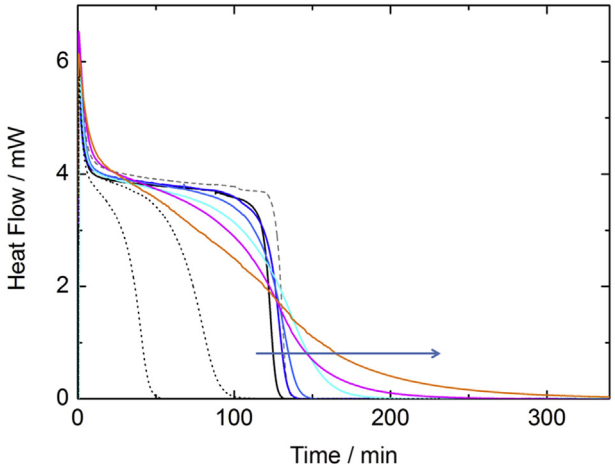

Fig. 1. Some examples of dehydration curves at 20 °C of PEG 600 solutions (12 mg loaded sample) with initial concentration ranging from 2 to 40% w/w. PEG concentrations (following the arrow) are 2, 5, 10, 20, 30, 40% w/w. Dot curves refer to water with 4, 8 and 12 mg loaded sample.

presented in Ref. [46], water activity, a_w, can be calculated as the ratio of HF(t)/HF(t = 0): here, HF(t = 0) is the intercept corrected for the calorimetric unbalance (see Fig. S3), HF(t) is the heat flow at time t, and the corresponding concentration at time t is evaluated from the amount of water evaporated as given by the partial integral of HF(t) vs t. Fig. 2 reports the values of a_w vs. water molar fraction, x_{H20}, for the series of solutions of Fig. 1, including some literature values of a_w for PEG 600 measured in the thermodynamic equilibrium with an AQUA-LAB dew point device (Decagon, USA), at 25 °C [48]. It is evident that literature values fully disagree from the spread of the calorimetric results obtained with solutions that, starting from an initial concentration ranging from 2% w/w to 40% w/w PEG 600, continuously undergo decrease in water concentration. Indeed, it is also clear that all the reported curves of a_w in Fig. 2 should collapse in one single curve fitting the literature data. Thus, some anomalous dependence of the experimental data as a function of the initial concentration loaded in the calorimeter appears.

At first glance, the simple hypothesis was made that PEG chains

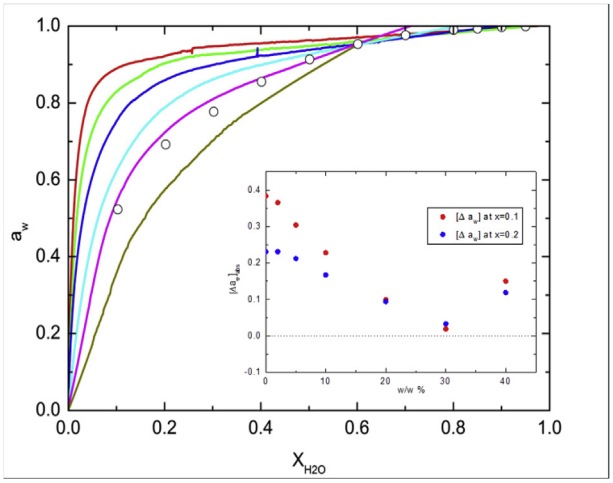

Fig. 2. Dependence of water activity, a_w, on water molar fraction, x_{H20}, for six representative samples of PEG 600 (initial concentration of dehydration process from 2% to 40% w/w PEG). Literature values of a_w for PEG 600 measured in the thermodynamic equilibrium are shown by circle data points [48]. Inset shows the deviation of water activity (Δa_w) at two x_{H2O} values (x_{H20} = 0.1 and 0.2) with respect to literature values, measured for the six solution at initial concentration from 2% to 40% w/w PEG.

could undergo a surface interaction within the cellulose micropores. Under these circumstances, the free concentration of PEG could have been affected up to the surface saturation. However, this hypothesis was discarded, since the existence of such an interaction seems debated in literature [49,50]. Assuming that no other artifacts affect the experiments, the spreading of the data away from the literature data could only be interpreted as a result of some failure in the "dynamic" calorimetry conditions when "low PEG concentrations" are used in the starting experiment. Thus, data from concentrated solution (here 30% w/w or more) should reflect a better solution homogeneity and equilibrium with respect to those of a dilute solution (2% w/w) which is subjected *in situ* to a rapid increase in solute concentration, without being able to continuously reset the solution equilibrium. Indeed, all polymer solutions are characterized by the so-called *coil-overlap critical concentration* which approximately marks two different rheological regimes. For the PEG solutions investigated, this threshold occurs at c* ~25% w/w (calculated from the unperturbed coil dimension of *ca.* 1 nm for PEG 600 [51]). Therefore, the more dilute solution (2% w/w) during an experimental time of about 2 h undergoes dehydration and increases its concentration by a factor of 50, crossing the critical concentration regime, while the more concentrated solution (40% w/w) is above this critical threshold c* and its concentration only increases by a factor of 2.5 in the same time. Although this observation does not directly imply the consequence of retarded dynamical phenomena, since other hidden processes may occur, still it represents a pitfall in the application of the dehydration theory previously presented. The spectroscopic results should more clearly detect this hallmark, while it is outside of the present study and requires further investigation the question about whether this dynamic behavior in PEG solution is coupled here also with some concentration gradient changes in confined cellulose micropores.

3.2. Ultraviolet Brillouin scattering

The collective dynamics of aqueous solutions of three PEG samples, namely, PEG 600, PEG 1000 and PEG 6000, have been studied in an unexplored frequency region ($\lambda = 220$ nm) as a function of temperature and concentration (See detail in Supplementary data). Compared to the visible, the UV region has the advantage to be able to follow the relaxation of water and water solutions at higher temperature, thus closer to physiological conditions [13]. The whole set of measurements is intended to disclose whether upon increasing concentration and molecular weight, while decreasing temperature, some changes in the structural relaxation could presage a different reorganization of the matrix, as it has been observed in highly hydrophilic systems [13]. IUVS spectra have been systematically recorded as a function of T encompassing the liquid and undercooled phases for each PEG sample solution, at monomer molar fraction x = 0.5, 0.33 and 0.1, as well as in water and in pure polymer (example of the fitting results is reported in Fig. S4).

Each set of experimental data shows a continuous change in both the inelastic peak angular frequency, ω, and the full width at half maximum (FWHM), Γ, as a function of concentration (Fig. 3) and temperature (data not shown). As a result, the data of Γ as a function of temperature (at constant concentration) show a characteristic dispersive trend illustrated in Fig. 4. In the explored temperature range, at low concentration ($x \leq 0.1$), only the final tail of the bell-shaped curve appears, while at given concentration (data with $x \geq 0.33$) Γ showed a clear maximum at a characteristic temperature, T_M (Fig. 4 left) in correspondence with the best experimental matching condition of the probed relaxation. The position of this relaxation maximum moves to higher temperatures upon increasing PEG concentration as an indication of the change of mobility of the system (Fig. 4 right).

Thus, Brillouin scattering data on aqueous PEG600 solutions in the UV range provide the values of the characteristic temperature, T_M, as precursor of the glass transition process at lower T (see Supplementary data Fig. S6).

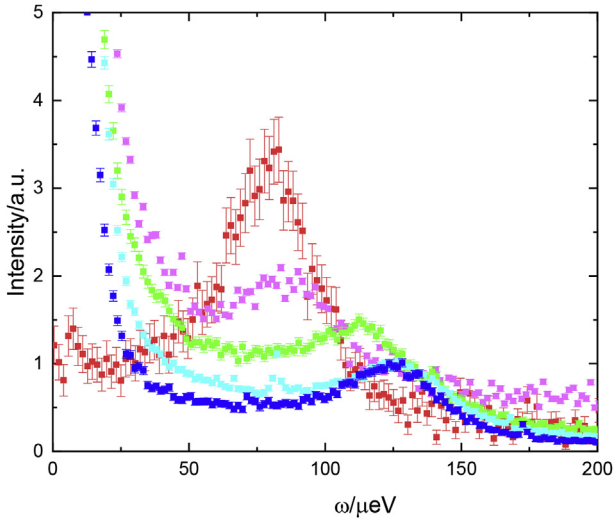

Fig. 3. Example of changes in frequency of the inelastic peak, ω, for PEG 600 solution with concentration x = 0 (red dots), x = 0.1 (pink dots), x = 0.33 (green dots), x = 0.5 (cyan dots), x = 1 (blue dots) at T = 25 °C. (For interpretation of the references to color in this figure legend, the reader is referred to the Web version of this article.)

It is worth noting that within the samples investigated, the values of Γ for samples PEG 600 and PEG 1000 coincide at all concentrations and temperatures, while PEG 6000 discloses some slight difference in the middle range of concentrations but not in pure polymer. Unfortunately, the accessible low temperature range was drastically limited for PEG 6000 in the pure or high concentration state because of the formation of the polymer crystalline phase.

A comment is deserved on the particular behavior of the dependence of T_g for a series of homologous polymer (PEG) reported by Faucher et al. [52] showing a distinct maximum in glass transition at about 6000 molecular weight. Given the strong kinetic character of the glass transition, this phenomenon has been correctly attributed to the high tendency to crystallize which reaches a maximum for samples with medium-low molecular weight. A related feature has been observed in the metastability of the PEG–water mixtures studied as a function of the molecular weight and of composition [53]. These findings are confirmed by the higher inflection point of the dispersion curve, i.e., the center of the viscoelastic crossover, revealing a distinctive solid-like behavior of PEG 6000 respect to PEG 600 at x = 0.33 and at x = 0.5, which is however negligible outside this concentration range at x = 1 or x = 0.1.

The relevance of these results is that water composition affects the conformational changes presaging the crystallization event which is evidently facilitated in samples with medium-low molecular weight. Although this phenomenon may deserve further investigation by viscoelastic and Brillouin experiments, a preliminary attempt to disclose a composition/conformation effect in the present Brillouin data can be made by using the values of the peak position ω as a function of composition (Fig. 5). At constant temperature, the addition of water to liquid PEG 600 first lead to a slight decrease and then to an increase in the solution viscoelastic relaxation. This behavior is consistent with the slowest polymer dynamics observed in the concentrated solution [32]. It is also worth mentioning that the results presented here substantially agree with other previous Brillouin studies [54–56], with visible radiation which reported extensive data aiming at correlating hydration and structural/dynamical effects in PEG 600 and PEG 400 or in low molecular weight samples (from 200 to 2000), but not encompassing the chain size anomaly.

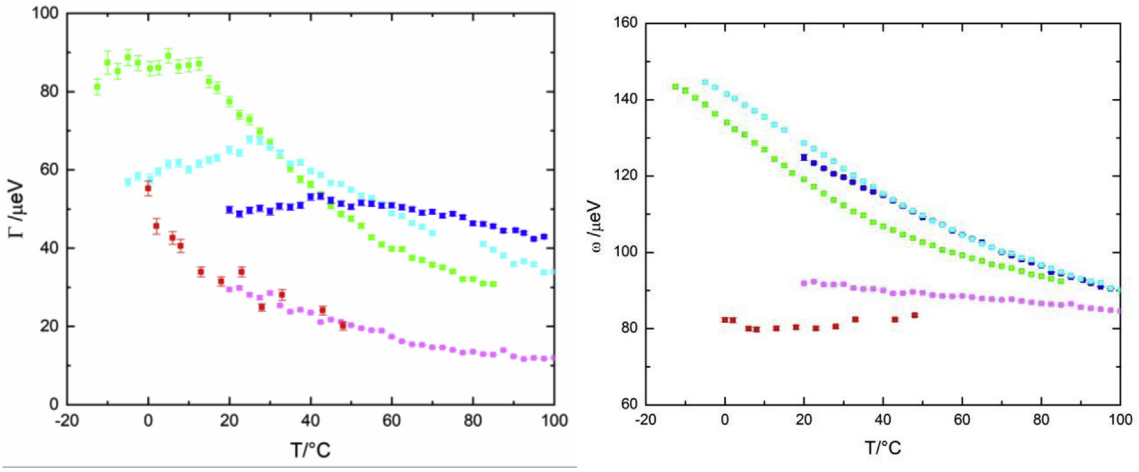

Fig. 4. Temperature behavior of the full width at half maximum, Γ, of the inelastic peak (left) and of the peak position ω (right). Concentrations: x = 0 (red dots), x = 0.1 (pink dots), x = 0.33 (green dots), x = 0.5 (cyan dots) and x = 1 (blue dots). (For interpretation of the references to color in this figure legend, the reader is referred to the Web version of this article.)

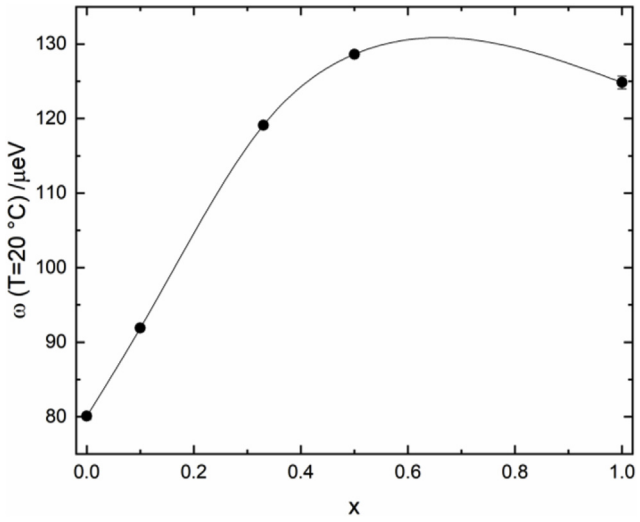

Fig. 5. Peak position ω at T = 20 °C as a function of the monomer molar fraction x (the line is guide for the eye only).

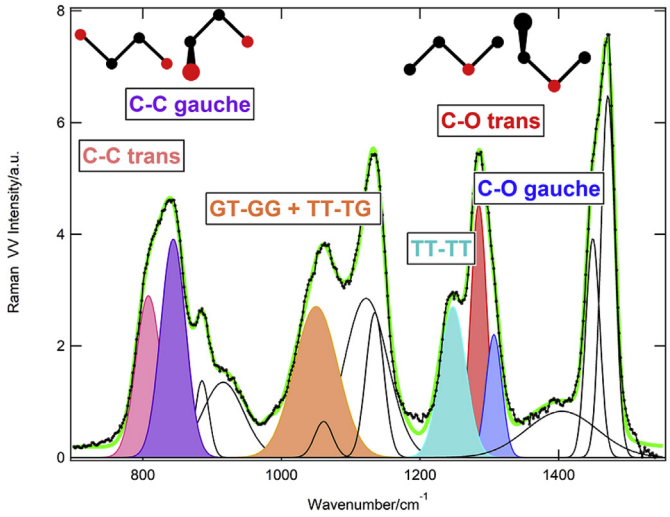

Fig. 6. Typical VV Raman spectrum of aqueous PEG 600 solution (here at monomer molar fraction x = 0.33, T = 57 °C). *Gauche* and *trans* conformational key bands for the C–C and the C–O bonds (see inserts) are indicated by colors as specified in the figure. Green curve represents the fit to the data, each band fitted with a Gaussian curve according to standard procedures. (For interpretation of the references to color in this figure legend, the reader is referred to the Web version of this article.)

3.3. Raman

The Raman study of the conformational behavior of PEG 600 as a function of concentration and temperature has been carried out by investigating the conformational key bands of the C–C bond in the *trans* and *gauche* conformations (800-850 cm^{-1}) and of the C–O bond the *trans* and *gauche* conformations (1280-1320 cm^{-1}) according to previous Raman wavenumbers observed in aqueous solutions and with the conformation assignment established since long time by normal coordinate analysis (ref. [57] Table III).

A typical example of the VV Raman spectra in the region between 700 and 1600 cm^{-1} of aqueous solutions of PEG with selected monomer mole fraction is shown in Fig. 6, where pink and violet band fill indicates the *trans* and *gauche* conformational key bands for the C–C bond and red and blue band fill indicates the *trans* and *gauche* conformational key bands for the C–O bond. Each band of the Raman spectra for different concentration and temperatures has been fitted with a Gaussian function, thus finding good agreement with the assignment of the vibrational bands which has been made for PEG by other authors [57–59].

Fig. 7 indicates that the intensity ratio of the *gauche* band relative to the *trans* band for the C–C bond decreases as a function of monomer mole fraction x by a factor of approximately 0.6–0.7 with a more accentuated drop above x = 0.33. On the contrary, the plot of the intensity ratio of the *gauche* band to the *trans* band for the C–O bond, also reported in Fig. 7, shows a small increase of the population of the *gauche* conformation with increasing monomer mole fraction x. Both trends are essentially in agreement with the literature [59]. Unfortunately, in the absence of an absolute standard, it is not possible to convert the intensity data in the corresponding numerical fraction of the *gauche* (and *trans*) conformation; nonetheless, the major contribution of water interaction in the stabilization of the *gauche* C–C conformation seems undiscussed, as indicated by the trend shown in Fig. 7. These results have the common interpretation in the greater accessibility of water to ether oxygen for the C–C gauche conformation.

Furthermore, it is worth mentioning that a characteristic shift up to ~8 cm^{-1} is detected for these peaks by increasing x values, from 0.1 to the melt (x = 1), with a different behavior for concentration and temperature changes (Fig. 8).

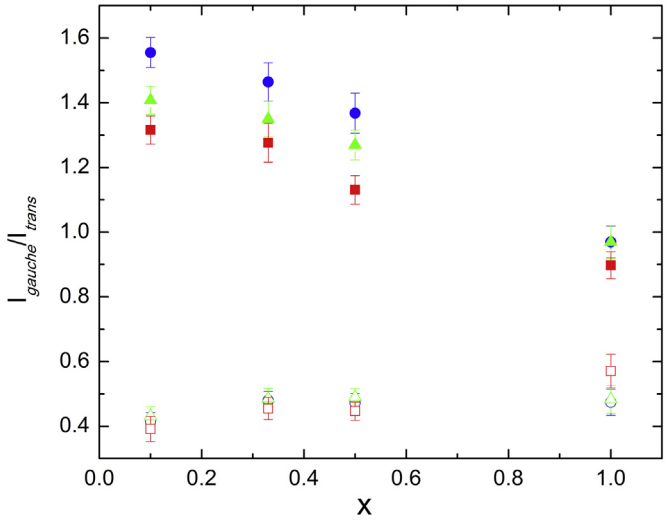

Fig. 7. Intensity ratio I_{gauche}/I_{trans} for the C–C bond (full symbols) and for the C–O bond (empty symbols) as a function of monomer molar fraction of PEG 600. Blue circles 27 °C, green triangles 57 °C, red squares 87 °C. (For interpretation of the references to color in this figure legend, the reader is referred to the Web version of this article.)

Indeed, there are many other features worth of mention in the C–O and the C–C peaks behavior in Fig. 8. First of all, the concentration dependence of the frequency for the C–O and C–C peaks depend on the temperature in a similar way for both *trans* and *gauche* conformations. In addition, the frequency changes with temperature in dilute solution (higher the temperature higher the frequency) are opposite to that of the pure liquid PEG (higher the temperature lower the frequency). Since the frequency value is straightforwardly associated to constrain of the surrounding, it is clear that the interplay of polar and non-polar interactions between water and PEG defines the opposite temperature derivative in Fig. 8 (left), with a temperature behavior independent of the conformation of the C–O bond (either *gauche* or *trans*). More importantly, these opposite frequency changes with temperature in the solution and in the melt determine also a rather unusual concentration independence observed for the frequency of C–O bonds around the physiological temperatures. In other words, around 37 °C there is little or no change of C–O hydration, showing the existence of a "buffered hydration" of PEG in the range of crowding conditions.

More regular is the change in frequency detected for the C–C peaks (either *gauche* or *trans*) as a function of concentration, with the low temperature frequencies always higher than the high temperature frequencies. Thus, the changes in these peaks constantly define a weaker constrain for decreasing water concentration.

The changes in local conformation and solvent interaction can be devoid of interest in the absence of information of the possible sequence, i.e., of the nearest-neighbor interactions affecting the long range conformational cooperativity. Unfortunately, no direct information on the Markoffian behavior of PEG chains in aqueous solution seems available in the literature. However, some indirect information can be obtained by the changes in vibrational peaks attributed to duplets or triplets containing well defined sequence of conformations. In particular, following the notation and the fragment identification by Matsuura and coworkers [57,59], the GT-GG and TT-TG conformations of the CH_2–CH_2–O–CH_2–CH_2 fragments at 1047-1053 cm^{-1} and the TT-TT conformation at 1243-1247 cm^{-1} have been considered. Thus, an overall decrease of the intensity ratio $(I_{GTGG} + I_{TT\text{-}TG})/I_{TT\text{-}TT}$ with increasing the monomer molar fraction of PEG 600 is observed at all temperatures (see Supplementary Data Fig. S7).

4. Conclusions

In the attempt to find evidence for a signature of concentration dependence of the PEG crowding features, aqueous solution properties were investigated by using experimental approaches ranging from the thermodynamic timescale to the Raman spectroscopy timescale,

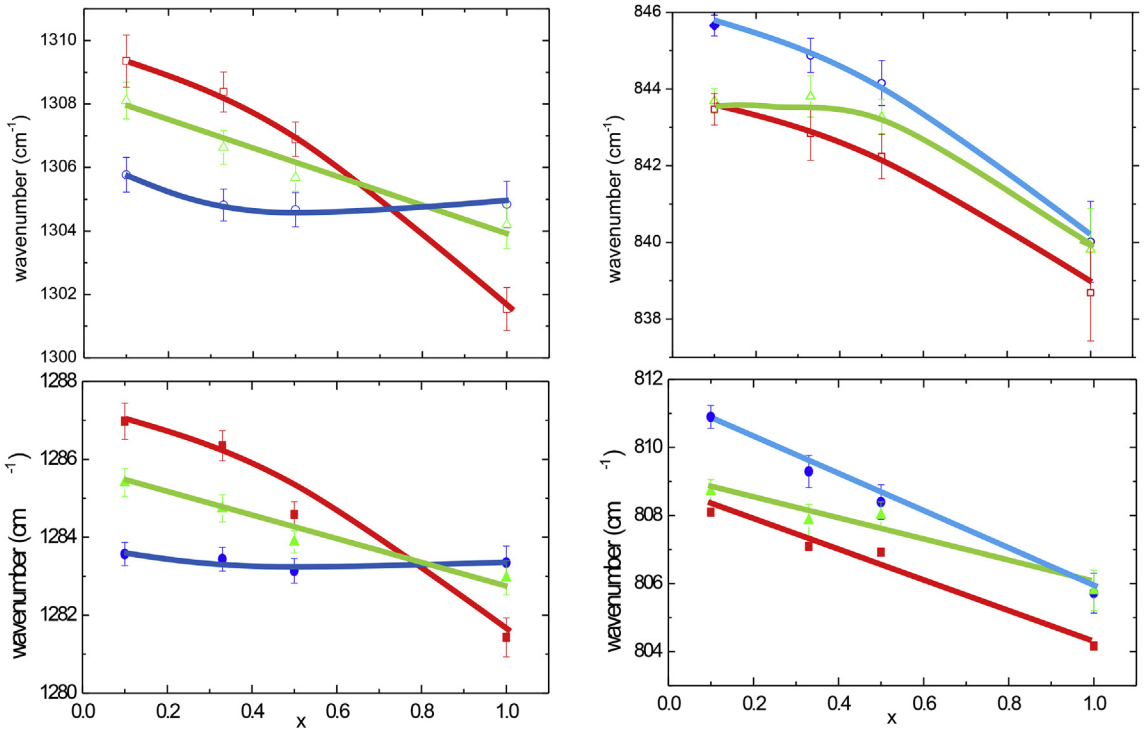

Fig. 8. Position for the band associated with the C–O (left) and C–C (right) bond conformation (empty symbols: *gauche;* full symbols: *trans*) as a function of monomer molar fraction of PEG 600 aqueous solution. Blue circles 27 °C, green triangles 57 °C, red squares 87 °C. Lines are a guide for the eye. (For interpretation of the references to color in this figure legend, the reader is referred to the Web version of this article.)

including Brillouin mesoscale. First, the water activity in aqueous PEG solution has been measured by a novel dynamic approach, revealing some non-equilibrium process for dilute solutions. Brillouin scattering data show the characteristic T_M which is the precursor of the glass transition process, with Tg ≈ T_M - 100 °C. At constant T (20 °C) the relaxation process monitored simply by peak position show two regimes at low and high water content. Some similar behavior is provided by the Raman bands intensities for gauche/trans conformations, evidencing changes in local and segmental conformations.

A scrutiny of the three properties reported here for PEG solutions show some common evidence for a sort of trend discontinuity around the concentration x ≈ 0.3–0.4 (see Figs. 2, 5 and 8). In particular, the results of Raman experiments clearly indicate that some non-linear changes in conformation occur, at physiological temperatures, as a function of concentration around x = 0.3–0.5. Similarly, above this concentration range the structural relaxation (here monitored by the ω value at 20 °C) starts to deviate from the almost linear trend shown at low concentration. Finally, isothermal dehydration experiments show that the rate of water removal does not always conform to that predicting the correct activity, but it depends on the actual concentration of the solution at time t = 0. This deviation is attributed to a still unclear process of non-homogeneous diffusion of PEG molecules at concentration below c* (for PEG 600 c* has been estimated around 25% w/w, i.e. x ≈ 0.15). Thus, it appears that water diffusion in the more homogeneous concentrated PEG solution provides an equilibrium value of the water activity. Indeed, several other literature data on water-PEG mixtures show a signature of strong interactions in the mentioned concentration range. In particular, it is worth mentioning the results of the excess volume [60] showing a remarkable negative minimum at x ca. 0.3, close to the eutectic point composition that reflects the maximum capacity of hydrogen bonding per monomer unit [52].

The implementation of the new data supports the idea that a water-mediated conformational change is the threshold for the transition from one regime to the other and vice-versa. The kinetic of this conformational transition depends on the water content and is of diffusive nature. The chain molecular size also influence this process with a counterbalancing effect at low molecular weight because of the liquid character prevalence and at high molecular weight because of the statistical random coil behavior. As a tentative conclusion, the crowding action seems best provided by a solution with a critical concentration of about 30% for a molecular weight of 600 Da, although validation is needed with more data. In particular, MD simulations to explore the coil dissymmetry plateau vs Mw and vs concentration would be useful to evidence the interplay between water hydration and local and long range conformational effects. Additional Raman experiments on dilute and semi-dilute PEG solutions of molecular weight from 200 to 20000 Da (i.e., with different c*) will have to be studied, especially to explore the observed conformational changes.

In conclusion, the heuristic overall result is that the multi-dimensional extended time-space domains approach suggests a quasi-regular solution behavior of PEG, with opposite concentration dependence at low and at high water content, similar to discontinuities observed in excess thermodynamic properties and eutectic phase diagram. The cross-over of these distinct behaviors depends on the timescale of the investigated but occurs at the concentration close to that usually employed to mimic the cellular crowding in biomolecular systems, highlighting the interplay of water molecules in solute-solute interactions as recently proposed for the interacting role of PEG with non-canonical G-quadruplex DNA [61].

Acknowledgements

The authors are indebted to BL10.2–IUVS Beamline scientists, for technical help during the Brillouin and Raman measurements. Support for computational work by CINECA ISCRA grants (Bologna, Italy) is gratefully acknowledged.

Appendix A. Supplementary data

Supplementary data to this article can be found online at https://doi.org/10.1016/j.polymer.2019.05.004.

References

[1] A.P. Minton, The effect of volume occupancy upon the thermodynamic activity of proteins: some biochemical consequences, Mol. Cell. Biochem. 55 (2) (1983) 119–140.
[2] T.C. Jarvis, D.M. Ring, S.S. Daube, P.H. Von Hippel, " Macromolecular crowding": thermodynamic consequences for protein-protein interactions within the T4 DNA replication complex, J. Biol. Chem. 265 (25) (1990) 15160–15167.
[3] A.A. Hyman, C.A. Weber, F. Jülicher, Liquid-liquid phase separation in biology, Annu. Rev. Cell Dev. Biol. 30 (2014) 39–58.
[4] R.J. Ellis, Macromolecular crowding: an important but neglected aspect of the intracellular environment, Curr. Opin. Struct. Biol. 11 (1) (2001) 114–119.
[5] R.C. Ford, S.V. Ruffle, A.J. Ramirez-Cuesta, I. Michalarias, I. Beta, A. Miller, J. Li, Inelastic incoherent neutron scattering measurements of intact cells and tissues and detection of interfacial water, J. Am. Chem. Soc. 126 (14) (2004) 4682–4688.
[6] S.I. Nakano, D. Miyoshi, N. Sugimoto, Effects of molecular crowding on the structures, interactions, and functions of nucleic acids, Chem. Rev. 114 (5) (2013) 2733–2758.
[7] R. Harada, Y. Sugita, M. Feig, Protein crowding affects hydration structure and dynamics, J. Am. Chem. Soc. 134 (10) (2012) 4842–4849.
[8] M. Gao, C. Held, S. Patra, L. Arns, G. Sadowski, R. Winter, Crowders and cosolvents—major contributors to the cellular milieu and efficient means to counteract environmental stresses, ChemPhysChem 18 (21) (2017) 2951–2972.
[9] M. Sumra Shahid, I. Hassan, A. Islam, F. Ahmad, Size-dependent studies of macromolecular crowding on the thermodynamic stability, structure and functional activity of proteins: in vitro and in silico approaches, Biochim. Biophys. Acta 1861 (2017) 178–197.
[10] P.K. Verma, A. Kundu, J.H. Ha, M. Cho, Water dynamics in cytoplasm-like crowded environment correlates with the conformational transition of the macromolecular crowder, J. Am. Chem. Soc. 138 (49) (2016) 16081–16088.
[11] X. He, A. Fowler, M. Toner, Water activity and mobility in solutions of glycerol and small molecular weight sugars: implication for cryo-and lyopreservation, J. Appl. Phys. 100 (7) (2006) 074702.
[12] F. Sussich, C. Skopec, J. Brady, A. Cesàro, Reversible dehydration of trehalose and anhydrobiosis: from solution state to an exotic crystal? Carbohydr. Res. 334 (3) (2001) 165–176.
[13] S. Di Fonzo, C. Masciovecchio, A. Gessini, F. Bencivenga, A. Cesàro, Water dynamics and structural relaxation in concentrated sugar solutions, Food Biophys. 8 (3) (2013) 183–191.
[14] M. Senske, L. Törk, B. Born, M. Havenith, C. Herrmann, S. Ebbinghaus, Protein stabilization by macromolecular crowding through enthalpy rather than entropy, J. Am. Chem. Soc. 136 (25) (2014) 9036–9041.
[15] P.J. Flory, Principles of Polymer Chemistry, Cornell University, Ithaca, 1953.
[16] L. Comez, M. Paolantoni, P. Sassi, S. Corezzi, A. Morresi, D. Fioretto, Molecular properties of aqueous solutions: a focus on the collective dynamics of hydration water, Soft Matter 12 (25) (2016) 5501–5514.
[17] J.M. Harris, S. Zalipsky, Poly(ethylene Glycol): Chemistry and Biological Applications, Am. Chem. Soc, Washington, DC, 1997.
[18] S. Šešlija, A. Nešić, J. Ružić, M.K. Krušić, S. Veličković, R. Avolio, G. Santagata, M. Malinconico, Edible blend films of pectin and poly (ethylene glycol): preparation and physico-chemical evaluation, Food Hydrocolloids 77 (2018) 494–501.
[19] K.A. Lyseng-Williamson, Macrogol (polyethylene glycol) 4000 without electrolytes in the symptomatic treatment of chronic constipation: a profile of its use, Drugs Ther. Perspect. 34 (2018) 300–310.
[20] EFSA Panel on Food Additives and Nutrient Sources added to Food (EFSA ANS Panel), Refined exposure assessment of polyethylene glycol (E 1521) from its use as a food additive, EFSA J. 16 (6) (2018) e05293.
[21] T.W.N. Bieze, A.C. Barnes, C.J.M. Huige, J.E. Enderby, J.C. Leyte, Distribution of water around poly (ethylene oxide): a neutron diffraction study, J. Phys. Chem. 98 (26) (1994) 6568–6576.
[22] M.P. Janelli, S. Magazu, G. Maisano, D. Majolino, P. Migliardo, Non-ideal compressibility in poly (ethylene oxide)-water solutions induced by H-bond interactions, J. Mol. Struct. 322 (1994) 337–343.
[23] G. Karlstrom, A new model for upper and lower critical solution temperatures in poly (ethylene oxide) solutions, J. Phys. Chem. 89 (23) (1985) 4962–4964.
[24] R. Kjellander, E. Florin, Water structure and changes in thermal stability of the system poly (ethylene oxide)–water, J. Chem. Soc., Faraday Trans. 1: Phys. Chem. Conden. Phas. 77 (9) (1981) 2053–2077.
[25] J.T. King, E.J. Arthur, C.L. Brooks III, K.J. Kubarych, Crowding induced collective hydration of biological macromolecules over extended distances, J. Am. Chem. Soc. 136 (1) (2014) 188–194.
[26] A. Rajapaksha, C.B. Stanley, B.A. Todd, Effects of macromolecular crowding on the structure of a protein complex: a small-angle scattering study of superoxide dismutase, Biophys. J. 108 (4) (2015) 967–974.
[27] F. Oesterhelt, M. Rief, H.E. Gaub, Single molecule force spectroscopy by AFM indicates helical structure of poly(ethylene-glycol) in water, New J. Phys. 1 (1999) 6.1–6.11.
[28] M. Grunze, A. Pertsin, L. Fabbrizzi, A. Poggi (Eds.), Molecular Conformations in Organic Monolayers Affect Their Ability to Resist Protein Adsorption, Springer-

Verlag, Berlin/Heidelberg, Germany, 2000.
[29] R.L.C. Wang, H.J. Kreuzer, M. Grunze, Molecular conformation and solvation of oligo(ethylene glycol)-terminated self-assembled monolayers and their resistance to protein adsorption, J. Phys. Chem. B 101 (1997) 9767–9773.
[30] R.L.C. Wang, H.J. Kreuzer, M. Grunze, The interaction of oligo(ethylene oxide) with water: a quantum mechanical study, Phys. Chem. Chem. Phys. 2 (2000) 3613–3622.
[31] K. Tasaki, Poly (oxyethylene) − water interactions: a molecular dynamics study, J. Am. Chem. Soc. 118 (35) (1996) 8459–8469.
[32] O. Borodin, D. Bedrov, G.D. Smith, A molecular dynamics simulation study of polymer dynamics in aqueous poly (ethylene oxide) solutions, Macromolecules 34 (16) (2001) 5687–5693.
[33] H. Lee, R.M. Venable, A.D. MacKerell Jr., R.W. Pastor, Molecular dynamics studies of polyethylene oxide and polyethylene glycol: hydrodynamic radius and shape anisotropy, Biophys. J. 95 (4) (2008) 1590–1599.
[34] H. Lee, A.H. de Vries, S.J. Marrink, R.W. Pastor, A coarse-grained model for polyethylene oxide and polyethylene glycol: conformation and hydrodynamics, J. Phys. Chem. B 113 (40) (2009) 13186–13194.
[35] R. Urbani, A. Cesàro, Solvent effects on the unperturbed chain conformation of polysaccharides, Polymer 32 (16) (1991) 3013–3020.
[36] H. Shin, T.A. Pascal, W.A. Goddard III, H. Kim, Scaled effective solvent method for predicting the equilibrium ensemble of structures with analysis of thermodynamic properties of amorphous polyethylene glycol–water mixtures, J. Phys. Chem. B 117 (3) (2013) 916–927.
[37] V.Y. Grinberg, T.V. Burova, N.V. Grinberg, A.S. Dubovik, V.S. Papkov, A.R. Khokhlov, Energetics of LCST transition of poly(ethylene oxide) in aqueous solutions, Polymer 73 (2015) 86–90.
[38] A. Azri, P. Giamarchi, Y. Grohens, R. Olier, M. Privat, Polyethylene glycol aggregates in water formed through hydrophobic helical structures, J. Colloid Interface Sci. 379 (1) (2012) 14–19.
[39] A. Azri, M. Privat, Y. Grohens, T. Aubry, Linear rheological properties of low molecular weight polyethylene glycol solutions, J. Colloid Interface Sci. 393 (2013) 104–108.
[40] S. Bandyopadhyay, M. Tarek, M.L. Lynch, M.L. Klein, Molecular dynamics study of the poly(oxyethylene) surfactant C12E2 and water, Langmuir 16 (3) (2000) 942–946.
[41] I.M. Kuznetsova, B.Y. Zaslavsky, L. Breydo, K.K. Turoverov, V.N. Uversky, Beyond the excluded volume effects: mechanistic complexity of the crowded milieu, Molecules 20 (1) (2015) 1377–1409.
[42] B. Bellich, E. Elisei, R. Heyd, M.L. Saboungi, A. Cesàro, Isothermal dehydration of thin films, J. Therm. Anal. Calorim. 121 (3) (2015) 963–973.
[43] https://www.elettra.trieste.it/lightsources/elettra/elettra-beamlines/iuvs/2018-01-25-21-05-44.html.
[44] B. Fåk, B. Dorner, Phonon line shapes and excitation energies, Phys. B Condens. Matter 234 (1997) 1107–1108.
[45] J.J. More, G.A. Watson (Ed.), The Levenberg-Marquardt Algorithm: Implementation and Theory. Numerical Analysis, Lecture Notes in Mathematics, Springer- Verlag, Berlin, 1977, pp. 105–116.
[46] R. Heyd, A. Rampino, B. Bellich, E. Elisei, A. Cesàro, M.L. Saboungi, Isothermal dehydration of thin films of water and sugar solutions, J. Chem. Phys. 140 (12) (2014) 124701.
[47] E. Gurian, B. Bellich, A. Cesàro, Polysaccharide solutions and gels: isothermal dehydration study by dynamic calorimetric experiments with DSC, Food Hydrocolloids 61 (2016) 163–171.
[48] L. Ninni, M.S. Camargo, A.J.A. Meirelles, Water activity in poly(ethylene glycol) aqueous solutions, Thermochim. Acta 328 (1–2) (1999) 169–176.
[49] D. Cheng, Y. Wen, L. Wang, X. An, X. Zhu, Y. Ni, Adsorption of polyethylene glycol (PEG) onto cellulose nano-crystals to improve its dispersity, Carbohydr. Polym. 123 (2015) 157–163.
[50] M.S. Reid, M. Villalobos, E.D. Cranston, The role of hydrogen bonding in non-ionic polymer adsorption to cellulose nanocrystals and silica colloids, Curr. Opin. Colloid Interface Sci. 29 (2017) 76–82.
[51] S. Hezaveh, S. Samanta, G. Milano, D. Roccatano, Molecular dynamics simulation study of solvent effects on conformation and dynamics of polyethylene oxide and polypropylene oxide chains in water and in common organic solvents, J. Chem. Phys. 136 (12) (2012) 124901 2012.
[52] J.A. Faucher, J.V. Koleske, E.R. Santee Jr., J.J. Stratta, C.W. Wilson III, Glass transitions of ethylene oxide polymers, J. Appl. Phys. 37 (11) (1966) 3962–3964.
[53] L. Huang, K. Nishinari, Interaction between poly(ethylene glycol) and water as studied by differential scanning calorimetry, J. Polym. Sci. B Polym. Phys. 39 (5) (2001) 496–506.
[54] C. Branca, S. Magazu, G. Maisano, F. Migliardo, P. Migliardo, G. Romeo, Hydration study of PEG/water mixtures by quasi elastic light scattering, acoustic and rheological measurements, J. Phys. Chem. B 106 (39) (2002) 10272–10276.
[55] M. Pochylski, F. Aliotta, Z. Blaszczak, J. Gapiński, Structuring effects and hydration phenomena in poly(ethylene glycol)/water mixtures investigated by Brillouin scattering, J. Phys. Chem. B 110 (41) (2006) 20533–20539.
[56] M. Pochylski, J. Gapinski, Brillouin scattering study of polyethylene glycol/water system below crystallization temperature, J. Phys. Chem. B 114 (8) (2010) 2644–2649.
[57] H. Matsuura, K. Fukuhara, Vibrational spectroscopic studies of conformation of poly (oxyethylene). II. Conformation–spectrum correlations, J. Polym. Sci. B Polym. Phys. 24 (7) (1986) 1383–1400.
[58] H. Matsuura, K. Fukuhara, Conformational analysis of poly(oxyethylene) chain in aqueous solution as a hydrophilic moiety of nonionic surfactants, J. Mol. Struct. 126 (1985) 251–260.
[59] R. Begum, H. Matsuura, Conformational properties of short poly(oxyethylene) chains in water studied by IR spectroscopy, J. Chem. Soc., Faraday Trans. 93 (21) (1997) 3839–3848.
[60] S.K. Begum, S.A. Ratna, R.J. Clarke, M.S. Ahmed, Excess molar volumes, refractive indices and transport properties of aqueous solutions of poly(ethylene glycol)s at (303.15–323.15) K, J. Mol. Liq. 202 (2015) 176–188.
[61] S. Di Fonzo, C. Bottari, J.W. Brady, L. Tavagnacco, M. Caterino, L. Petraccone, J. Amato, C. Giancola, A. Cesàro, Crowding and conformation interplay on human DNA G-quadruplex by ultraviolet resonant Raman scattering, Phys. Chem. Chem. Phys. 21 (2019) 2093–2101 2019.